ResearchGate

See discussions, stats, and author profiles for this publication at: https://www.researchgate.net/publication/317210025

The effort of the dynamic simulation on the fatigue damage evaluation of flexible mechanical systems loaded by...

Article *in* International Journal of Fatigue · October 2017

DOI: 10.1016/j.ijfatigue.2017.05.020

CITATIONS
0

READS
20

5 authors, including:

Filippo Cianetti
Università degli Studi di Perugia

96 PUBLICATIONS **312** CITATIONS

SEE PROFILE

Massimiliano Palmieri
Università degli Studi di Perugia

3 PUBLICATIONS **1** CITATION

SEE PROFILE

Janko Slavič
University of Ljubljana

67 PUBLICATIONS **474** CITATIONS

SEE PROFILE

Claudio Braccesi
Università degli Studi di Perugia

86 PUBLICATIONS **316** CITATIONS

SEE PROFILE

Some of the authors of this publication are also working on these related projects:

Project SOFTWIND - Smart Optimized Fault Tolerant WIND turbines - PRIN2015 View project

Project Electromagnetic Sources of Noise View project

All content following this page was uploaded by Filippo Cianetti on 30 May 2017.

The user has requested enhancement of the downloaded file. All in-text references underlined in blue are added to the original document and are linked to publications on ResearchGate, letting you access and read them immediately.

International Journal of Fatigue xxx (2017) xxx-xxx

Contents lists available at ScienceDirect

International Journal of Fatigue

journal homepage: www.elsevier.com

Technical note

The effort of the dynamic simulation on the fatigue damage evaluation of flexible mechanical systems loaded by non-Gaussian and non stationary loads

F. Cianetti[a, *], M. Palmieri[a], J. Slavič[b], C. Braccesi[a], G. Morettini[a]

[a] University of Perugia, Department of Engineering, Via G. Duranti 93, 06125 Perugia, Italy
[b] University of Ljubljana, Faculty of Mechanical Engineering, Askerčeva 6, 1000 Ljubljana, Slovenia

ARTICLE INFO

Article history:
Received 17 March 2017
Received in revised form 22 May 2017
Accepted 24 May 2017
Available online xxx

Keywords:
Vibration fatigue
Flexible components
Dynamic simulation
Non-stationary signals
Non-Gaussian signals

ABSTRACT

Even if in fatigue application it is common to assume stationary and Gaussian excitation, the impact of non-Gaussian and non-stationary loadings on the service life of a mechanical component is known. Non-Gaussian and non-stationary excitations are generally observed in several industrial applications (i.e. automotive, aeronautical, etc.) and for this, the assessment of the effect of such loads results necessary. From this assumption, the activity herein presented starts from experimental results, previously obtained, that analysed the influence of non-Gaussianity (generally evaluated by kurtosis) and of non-stationarity of inputs on the fatigue life of an Y-shaped specimen. In the present paper the finite element model of the sample and its full validation obtained by numerical/experimental comparison is presented. Moreover, due to the relevant effect of the system's dynamics on the stress/strain response previously observed, a wider assessment of non-Gaussianity and non-stationarity influence on the fatigue life has been numerically analysed together with the influence of the multi modal behaviour of the component by adopting an excitation frequency range that excites two modes of the model.

© 2017 Published by Elsevier Ltd.

UNCORRECTED PROOF

1. Introduction

In recent years, the design of mechanical components required on one side reliable results, and on the other short computational time. The frequency domain approach for the fatigue life estimation is increasing due to the required short computational time. By the above approach, random processes are treated through a spectral representation: a power spectral density (PSD) [1,2] is used to characterize the random load and to estimate the distribution of the rainflow cycles distribution [3]. Several methods for damage evaluation in frequency domain have been developed in the last thirty years [4–6].

Majority of the frequency domain methods available in literature are implicitly based on the hypothesis of Gaussianity of the input, that is, according to the linear behaviour of the system, on the Gaussianity of the stress PSD function (output). However, in fatigue analysis it is common to deal with structures subjected to non-Gaussian and non-stationary loads. In industrial application, such as automotive [7] (*i.e.* road irregularities) or wind turbine [8] (*i.e.* wind) or in aeronautics applications [9,10] (*i.e.* pressure fluctuations) the assumption of Gaussianity of the input cannot always be made.

For these reasons, the non-Gaussianity and non-stationarity have been subjected of several studies in recent years. Wolfsteiner [11], developed a new methodology for the decomposition of a non-stationary random vibration signal into a combination of several different stationary Gaussian signal, in order to make a correct frequency domain based fatigue load calculation.

Moreover, since the non-Gaussianity is often identified through two parameters, called kurtosis and skewness [12], Rizzi et al. [13] and Kihm et al. [14] investigated how the kurtosis influences the fatigue life of linear and non-linear system. They have demonstrated that, in linear regime, non-Gaussian loads produce Gaussian responses due to the respect of the central limit theorem (CLT) [1], while in case of non-linear regime, all response are non-Gaussian, because the CLT requirement is violated.

Furthermore, several studies have been conducted in order to determine the possibility to adapt, in different ways, the standard frequency methods also in case of structures subjected to non-stationary non-Gaussian excitations. Benasciutti et al. [15] computed a comparison between the results obtained with the Tovo-Benasciutti method (TB) [16], and the well-known narrow-band method in case of stationary non-Gaussian excitations, certifying that the TB method is able to consider the non-Gaussianity effects, while the narrow-band approximation gives unreliable results.

Braccesi et al. [17], instead, determined a correction coefficient as function of the kurtosis and the skewness of the stress process and of the S-N fatigue strength, which allows to correct the fatigue damage, evaluated under the Gaussian hypothesis. This approach was investigated by Niesłony [18], which certified that, in case of non-zero mean stress non-Gaussian time histories, the use of spectral methods, with the correction coefficient proposed by Braccesi et al. [17], leads to accurate results.

* Corresponding author.
Email address: cianfi@unipg.it (F. Cianetti)

http://dx.doi.org/10.1016/j.ijfatigue.2017.05.020
0142-1123/© 2017 Published by Elsevier Ltd.

A previous activity conducted by Palmieri et al. [19], experimentally investigated the influence of the kurtosis on the fatigue life of a unimodal flexible linear system. It was experimentally confirmed that in the case of stationary non-Gaussian loads, the response of the structure becomes Gaussian due to the dynamic behaviour of the system, while in case of non-stationary non-Gaussian excitations the system is not sufficiently dynamically excited and, for this reason, the response remains non-Gaussian with the same kurtosis of the input. The influence of non-Gaussianity was experimentally investigated with a set of non-Gaussian excitations, made up of stationary non-Gaussian signals with kurtosis 5.5 and 7, and non-stationary non-Gaussian excitation with kurtosis 7, by adopting a flat PSD aimed to only excite one mode [19].

In the present research, the influence of non-stationarity and of non-Gaussianity is numerically investigated, both in time and frequency domain. The finite element model of the sample, adopted in the previous and in the present activity, and its full validation obtained by numerical/experimental comparison is presented. A larger set of stationary and non-stationary non-Gaussian excitations was used in order to evaluate the impact of the kurtosis on the fatigue life (of a linear flexible system).

Moreover, compared to the research by Palmieri et al. [19], a step forward was made by extending the analysis to a multimodal flexible behaviour by adopting an excitation frequency range that excites two modes of the model.

The influence of non-stationarity and of non-Gaussianity is investigated through the evaluation of the kurtosis and skewness of the response in terms of stress state. As stated before, the fatigue life is evaluated in time domain by the rainflow counting approach [3], while in frequency domain by the Dirlik method [4]. The results obtained in time domain are considered as reference.

In such a way, it has been possible to determine the accuracy of the frequency methods for the damage evaluation in case of stationary and non-stationary Gaussian and non-Gaussian excitations, certifying in what condition the approximation to consider a non-Gaussian load as Gaussian, approaching the problem directly in frequency domain, allows to obtain accurate results.

The manuscript is organized as follow. In Section 2 theoretical aspects about random signals, dynamics stress recovery and damage evaluation are presented. In Section 3 the influence of component dynamics into fatigue damage evaluation was studied starting from a component finite element model and by performing dynamic simulations in time and frequency domain. A lot of input signals were considered characterized by different Gaussian or non-Gaussian, stationary or non-stationary characteristics. Section 4 draws the conclusion.

2. Theoretical background

In vibration fatigue, different aspects have to be considered [20]. Firstly, the assessment of the mechanical component loads is required. As those loads are frequently random, the signal processing knowledge is required [1]. Secondly, due to the influence of the dynamics on the system's response, a theoretical knowledge of the impact on results, that the dynamic behaviour of flexible bodies (structural dynamics) has, is necessary [2]. Moreover, once the stress in the most damageable location is known, the accumulated damage can be determined with different methods available in literature [2,4–6,20].

2.1. Random loads

Generally, in fatigue application is common to deal with structures subjected to random loads. As known, a generic signal can be categorized into deterministic or stochastic (random) signals. Since in vibration fatigue structures are subjected to time varying excitations, these processes are treated with the probabilistic approach [2].

A random signal x is described by the probability density function (PDF) as function of the random variable itself and of the time (t):

$$p(x,t) = \lim_{\Delta x \to 0} \frac{Prob[x<x(t) \leqslant x + \Delta x]}{\Delta x} \tag{1}$$

The central moments associated to a probability distribution characterize the properties of the distribution itself [1,2]. The j-th central moments M_j is defined as:

$$M_j = \frac{1}{n}\sum_{i=1}^{n}(x_i(t) - \mu(t))^j \tag{2}$$

The first and the second central moments are respectively the mean value and the variance, defined as follows:

$$\mu(t) = \frac{1}{n}\sum_{i=1}^{n} x_i(t) \tag{3}$$

$$\sigma^2(t) = \frac{1}{n}\sum_{i=1}^{n}\left(x_i(t) - \mu(t)\right)^2 \tag{4}$$

where n is the number of points in the sample time history record. If the random process is Gaussian the $p(x,t)$ takes the form:

$$p(x,t) = \left[\sigma(t)\sqrt{2\pi}\right]^{-1} e^{\frac{-[x-\mu(t)]^2}{2\sigma^2(t)}} \tag{5}$$

In engineering practice, it is common to assume a Gaussian probability distribution for several reasons: firstly, a real process assumes generally a Gaussian distribution and secondly, the consideration of a Gaussian random load allows to simplify the problem ensuring a good reliability.In some cases, such as in vehicle application [7] or in train application [21] or in aerospace application (*i.e.* pressure fluctuation) [9,10], the assumption of Gaussian load cannot be made. The non-Gaussianity of random process is defined by two parameters namely kurtosis k_u and skewness s_k respectively. These parameters are used to characterize the non-Gaussianity of a signal and they are identified in terms of the central moments as follows:

$$k_u = \frac{M_4}{M_2^2} = \frac{M_4}{\sigma^4} \qquad s_k = \frac{M_4}{M_2^{3/2}} = \frac{M_4}{\sigma^3} \tag{6}$$

The kurtosis characterizes the sharpness of the PDF peak and the width of the PDF tails. The skewness is a measure of the asymmetry of the PDF. The kurtosis of a Gaussian distribution is 3 while the skewness is 0; and a process is regarded to be leptokurtic if its kurtosis is higher than 3, and platykurtic if it is smaller than 3 [2].

It has been established how both, kurtosis and skewness, affect the fatigue life of a mechanical component, and moreover, it has been

UNCORRECTED PROOF

probed how an increase of the kurtosis leads to an increase of the accumulated damage within a structure [17].

2.2. Dynamic of structures

As known, the equation of motion for a multi-degree of system (MDOF), with n degrees of freedom, can be written as follows:

$$[M]\{\ddot{\delta}\} + [C]\{\dot{\delta}\} + [K]\{\delta\} = \{f\} \tag{7}$$

where $[M]$ is the mass matrix $(n \times n)$, $[C]$ is the damping matrix $(n \times n)$ and $[K]$ is the stiffness matrix $(n \times n)$, respectively. Vector $\{\delta\}$ represents the displacement of the system degrees of freedom $(n \times 1)$, while the vector $\{f\}$ represents the vector of force $(n \times 1)$ as the input to the system.A useful representation of Eq. (7) arises by a modal decomposition [2]. Indeed, considering the linear transformation $\{\delta\} = [\Phi]\{q\}$, where $\{q\}$ is a vector of dimension $(n \times 1)$ representing the generalized coordinates and $[\Phi]$ is the modal matrix of dimension $(n \times n)$, it is possible to write:

$$[I]\{\ddot{q}\} + [2\xi\omega_0]\{\dot{q}\} + [\omega_0^2]\{q\} = [\Phi]^{\mathrm{T}}\{f\} \tag{8}$$

where the matrix $[I]$ $(n \times n)$ is the identity matrix, the matrix $[2\xi\omega_0]$ is a diagonal matrix of damping of dimension $(n \times n)$ in which ξ represents the damping ratio, while $[\omega_0^2]$ is the diagonal matrix of eigenvalues of dimension $(n \times n)$.

In case that only m modes are considered, the matrix $[\Phi]$ has dimension $(n \times m)$ while $\{q\}$ has dimension $(m \times 1)$ and consequently also the matrix $[2\xi\omega_0]$ and $[\omega_0^2]$ have dimension $(m \times m)$. In the hypothesis of linear behaviour of the system, it is possible to adopt a state space representation which allows to reduce the order of the equation system. This approach allows to correctly simulate the dynamic of the system both in time domain and frequency domain.

By the state space approach [22], Eq. (8) can be re-written as follows:

$$\begin{aligned} \{\dot{z}(t)\} &= [A]\{z(t)\} + [B]\{u(t)\} \\ \{y(t)\} &= [C]\{z(t)\} + [D]\{u(t)\} \end{aligned} \tag{9}$$

Eq. (9) is the classical representation of the state space approach defined by the matrix $[A]$ (state to state), $[B]$ (input to state), $[C]$ (state to output) and $[D]$ (input to output) in the hypothesis of a system with $\{u\}$ input and $\{y\}$ output. The state space matrix has dimension $[A]$ $(2m \times 2m)$, $[B]$ $(2m \times p)$, $[C]$ $(m \times 2m)$ and $[D]$ $(m \times p)$ where m is the number of the considered modes and p represents the number of input while the state vector $\{\dot{z}(t)\} = \left\{\begin{matrix}\{\dot{q}\}\\\{\ddot{q}\}\end{matrix}\right\}$ has dimension $(2m \times 1)$, $\{u(t)\}$ has dimension $(p \times 1)$ and $\{y(t)\}$ has dimension $(m \times 1)$ respectively. Considering the 2nd hypothesis that the input to the system is a force, the state space matrix $[A]$ and $[B]$ take the form:

$$[A] = \begin{bmatrix} [0] & [I] \\ [\omega_0^2] & -[2\xi\omega_0] \end{bmatrix} \qquad [B] = \begin{bmatrix} [0] \\ [\Phi]_{inp}^T \end{bmatrix} \tag{10}$$

where $[\Phi]_{inp}^T$ is a matrix of dimension $(m \times p)$, representing a submatrix of the only degree of freedom that will be loaded by the input force. In such way, by coupling the state space approach and the modal approach, it is possible to obtain the so-called modal state space [23,24] which simply allows to approach the problem in time and frequency domain, since it requires only a subset of eigenvalues and of mode shapes and the damping ratio.

The matrix $[C]$ and $[D]$ instead depend on the required output. Indeed, in case the required outputs are the modal coordinates $\{q\}$, these matrix take the form:

$$[C] = \begin{bmatrix}[1] & [0]\end{bmatrix} \qquad [D] = \tag{11}$$

2.3. Stress recovery

Once the system has been represented with the modal state space shown in Section 2.2, it is possible to perform the fatigue analysis both in time and in frequency domain. For the time domain approach load time histories have to be defined and the state space system has to be computed by numerical integration. Once the time history of $q(t)$ is obtained (9), the time history of stress can be easily obtained for a single element through a linear combination:

$$\{\sigma(t)\} = [\Phi]^{\sigma}\{q(t)\} \tag{12}$$

where $[\Phi]^{\sigma}$ is the modal stress matrix $(6 \times m)$ of the single element. The stress recovery step (12) can be made for all the elements but also limited to a subset of them, for example for those located in the most damageable areas. The stress modal matrix is an accessory result of the same modal analysis performed to build the state space model (10).

In order to evaluate the damage within a structure, in case of multiaxial stress state, different approaches can be used [20]. In this work, the equivalent uniaxial approach, as proposed by Braccesi et al. [25], is used.

Once the equivalent uniaxial stress time history is known, in order to assess the cumulated fatigue damage, it is necessary to compute the probability density function of stress amplitude $f_{\sigma}(\Delta\sigma)$. For the probability density function different approaches are possible; here the rainflow counting method [3] is used.

In order to perform the damage evaluation in frequency domain, the stress PSD functions matrix (6×6) has to be obtained for each element. To this aim it is necessary to define the matrix of frequency response functions $[H_q](m \times p)$ between the p generic inputs and the m outputs [1,2], that are the Lagrangian coordinates from the modal state space representation (see Section 2.2). The matrix $[H_q]$ can be determined as follows [22]:

$$[H_q] = [C] \cdot (j\omega[I] - [A])^{-1}[B] \tag{13}$$

Therefore, by the assessment of the input power spectral density $G_x(\omega)$ of dimension $(p \times p)$, it is possible to obtain the power spectral density of the generalized coordinates $[G_q(\omega)]$ as follows:

$$[G_q(\omega)] = [H_q]\left[G_x(\omega)\right][H_q]^T \tag{14}$$

Once the power spectral density $[G_q(\omega)]$ is known, the power spectral density functions matrix of the stress tensor $[S]$ of dimension (6×6) for a single element can be obtained from the following rela-

UNCORRECTED PROOF

tion:

$$[S(\omega)] = [\Phi]^{\sigma}\left[G_q(\omega)\right][\Phi]^{\sigma,T} \tag{15}$$

In order to perform a fatigue analysis in case of multiaxial stress state in frequency domain, several methods are available in literature. In this activity, the power spectral density of the equivalent stress proposed by Premount (EQVM) [26] is used:

$$S_{eq}(\omega) = Trace[[Q][S]] \tag{16}$$

In Eq. (16) $[Q]$ is a constant matrix, which, for a planar stress state, is given by:

$$[Q] = \begin{bmatrix} 1 & -1/2 & 0 \\ -1/2 & 1 & 0 \\ 0 & 0 & 3 \end{bmatrix} \tag{17}$$

Using this definition, the equivalent stress PSD $S_{eq}(\omega)$ is a stationary zero-mean Gaussian process [26,27]; therefore, the existing frequency methods for the so called direct fatigue life calculation can be used [28].

The damage evaluation in frequency domain arises from the evaluation of the stress cycles distribution $f_\sigma(\Delta\sigma)$ that may be computed, for example, with the formulation proposed by Dirlik [4]:

$$f_\sigma(\Delta\sigma) = \frac{\frac{D_1}{Q}e^{(-Z/Q)} + \frac{D_2 Q}{R^2}e^{-(Q^2/(2R^2))} + D_3 Z e^{(-Q^2/2)}}{2\sqrt{m_0}} \tag{18}$$

where

$$\gamma = m_2/\sqrt{m_0 m_4} \qquad R = (\gamma - x_m - D_1^2)/(1 - \gamma - D_1 + D_1^2)$$

$$Z = \Delta\sigma/(2\sqrt{m_0}) \qquad D_2 = (1 - \gamma - D_1 - D_1^2)/(1 - R)$$

$$x_m = (m_1/m_0)\sqrt{m_2/m_4} \qquad D_3 = (1 - D_1 - D_2)$$

$$D_1 = [2(x_m - \gamma^2)]/(1 + \gamma^2) \qquad Q = 1.25\cdot(\gamma - D_3 - D_2 R)/D_1$$

and where the following equation:

$$m_n = \int_0^\infty \omega^n S_{eq}(\omega)d\omega \tag{19}$$

defines the n-th spectral moment of the signal.

2.4. Damage evaluation

From the knowledge of the stress range probability density function in time or in frequency domain, and from the knowledge of the fatigue strength curve of the material (*i.e.* in the stress domain $S-N$), it is possible to calculate the fatigue damage by adopting a cumulative damage law (*i.e.* linear cumulative damage law of Palmgren-Miner [29]).

For the $S-N$ curve, the following formulation is used:

$$\Delta\sigma^k = \frac{C}{N} \tag{20}$$

where N is the number of load cycles, k is the curve slope and C is the curve intercept.

Alternatively, the Basquin equation [29,30] formula can be used:

$$N = \left(\frac{\sigma_a}{\alpha}\right)^{1/\beta} \tag{21}$$

where σ_a is the amplitude of the applied load ($\sigma_a = \frac{1}{2}\Delta\sigma$), β is the curve slope and α is the curve intercept.

The parameters k and C are related to the parameters α and β by the following relations: $\beta = -1/k$ and $\alpha = \frac{1}{2}C^{-\beta}$.

For a random stress process, the fatigue damage D can be computed with the Palmgren-Miner law [29] by the following relation::

$$D = \frac{n}{C}\int_0^{+\infty}(\Delta\sigma)^k f_\sigma(\Delta\sigma)d(\Delta\sigma) \tag{22}$$

In Eq. (22), $f_\sigma(\Delta\sigma)$ represents the probability density function (PDF) of the stress cycles and n is the applied load cycles number related to a given applied stress amplitude

3. Vibration fatigue vs. stationarity and Gaussianity

The most evident effort of the frequency domain evaluation of damage is the reduction of computational time both in terms of dynamic simulation and stress recovery (see Section 2.3) and in terms of damage evaluation (see Section 2.4). If the stress state shows itself as Gaussian this is a valid alternative respect the reference time domain approach that requests huge computational times.

As concerns damage (fatigue) evaluation, all the frequency methods start from the assumption that the input excitation is both Gaussian and stationary. In order to estimate the damage also in case of non-Gaussian loads, different methods are presented in literature. The method used in this activity consists to correct the calculated damage, determined with the standard Gaussian-based frequency method, with a correction coefficient. In fact, the damage caused by a non-Gaussian input D_{ng} can be obtained by multiplying the Gaussian damage, D_g, which is known if the PSD of stress is known, with a correction coefficient λ_{ng}. In this manner, the damage for a non-Gaussian stress condition can be determined as follows:

$$D_{ng} = \lambda_{ng} D_g \tag{23}$$

UNCORRECTED PROOF

In this activity, the formula proposed by Braccesi et al. [17] for the non-Gaussian coefficient is used:

$$\lambda_{ng} = e^{\frac{m^{3/2}}{\pi}\left(\frac{(k_u-3)}{5}-\frac{s_k^2}{4}\right)} \tag{24}$$

The non-Gaussian coefficient λ_{ng} of Eq. (24) is a function of the kurtosis k_u, of the skewness s_k of the stress response and of the S-N curve slope m. As obvious, this approach imposes the assessment of the stress response in time domain. But as demonstrate by authors [17,31] in order to estimate stress state kurtosis and skewness a shorter numerical analysis or a shorter experimental record is required respect to those required to obtained a stabilised value of damage. This result have suggested to combine frequency domain evaluation of damage (to obtain Gaussianity effort) and time domain non-Gaussianity evaluation (kurtosis and skewness) [17] (hybrid approach).

As concerns dynamics, Palmieri et al. [19] experimentally researched the influence of non-Gaussianity and of non-stationarity of a linear flexible system (Fig. 1). In that activity several random loads stationary with kurtosis 3, 5.5 and 7 and non-stationary with kurtosis 7 for three different RMS values were generated from the same constant PSD function [19]. To obtain the condition of a flexible component excited in the range of its natural frequencies and in particular the excitation of a single mode of the specimen, the input PSD function was designed with a frequency range from 600 to 850 Hz. Under those test conditions, the obtained results certified how in case of stationary excitations, Gaussian or non-Gaussian, the response of the system was always stationary Gaussian and for this, the fatigue life obtained experimentally and numerically with for example the TB method [16], were comparable to each other. Instead, for the case of non-stationary excitation the system's stress response remained non-stationary non-Gaussian, and the computed fatigue life was significantly different if compared to the experimental one.

The same activity has showed as the kurtosis output (with input signals characterized by skewness equal to zero) assume a value equal at most to the inputs kurtosis and, from engineering point of view, this means that in design phase, in presence of non-stationary input signals, the non-Gaussianity could be evaluated only by analysing inputs and avoiding the short time domain simulation of the hybrid approach. This should allow to obtain a fatigue damage evaluation in a very short time.

The present research starts from the above activity and related results [19]. The same specimen was numerically analysed exciting more than one normal mode and adopting a larger set of random loads. The aim was to numerically investigate the influence of non-Gaussianity and of non-stationarity of loads and to examine the influence of the dynamics on the system's response establishing, with greater certainty, under which conditions it is allowed to ignore the non-Gaussianity of the inputs. Moreover, another aim was to evaluate the confidence of the proposed hybrid approach in evaluating damage when compared with the time domain approach (called "real damage").

3.1. Description of the specimen test conditions and of its dynamic modelling

The specimen adopted in this activity is a Y-shaped one, shown in Fig. 1. The geometry of the specimen consists of two main beams that are arranged at 120° angles, around the main axis, and have a rectangular cross section of 10×10 mm. Moreover, two inertial weights can be installed at the end of each arm in order to adjust its dynamic behaviour (i.e. natural frequencies). The Y-shaped specimen was made from the aluminium alloy A-S8U3 with a Young Modulus E = 75,000 MPa and density $\rho = 2710\ \mathrm{kg/mm^3}$. The material fatigue parameters were experimentally determined through a numerical minimization of the sum of the squared difference between the estimated and the experimental fatigue life [19]. The Basquin's equation can be written as follows:

$$\sigma_a = 987.5 \cdot N^{-0.169} \tag{25}$$

A finite element model was realized. It is shown in Fig. 2 and it consists of 15,600· 10-node tetrahedral elements. Moreover, in order to reduce the computational time, Shell "skin" element with a thickness of 1×10^{-6} mm were applied at the external surface of the

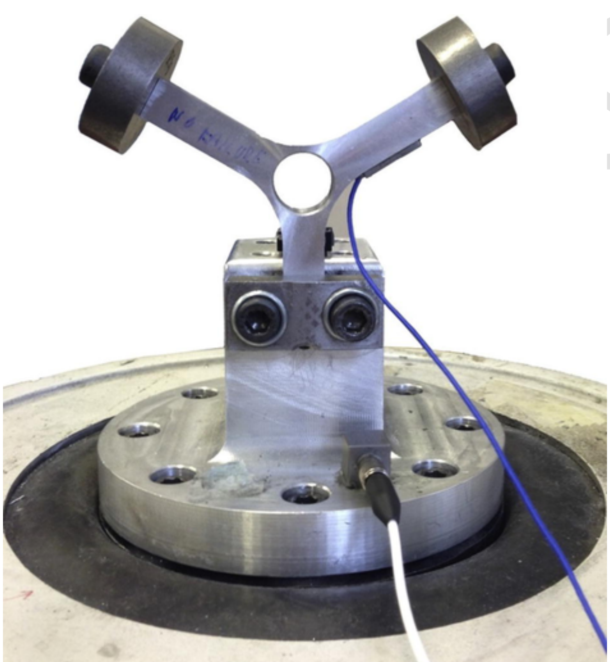

Fig. 1. Specimen and experimental tests configuration [19].

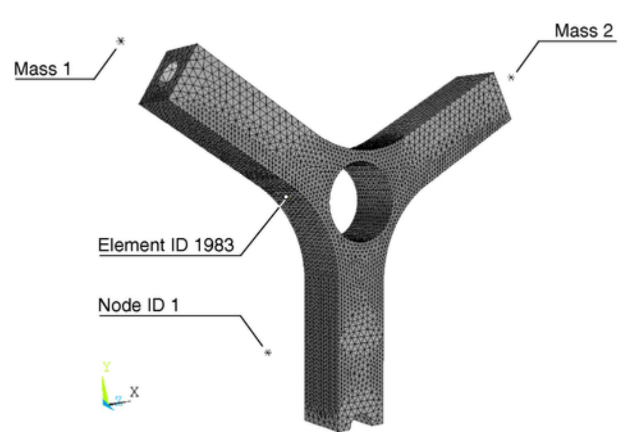

Fig. 2. Specimen finite element model (FEM).

model and the modal stress shapes $[\Phi]^{\sigma}$ were extracted only for those elements. The two inertial weights were modelled by point mass elements.

The goodness of the numerical model and of the state space modelling of its dynamic behaviour has been previously verified through a numerical and experimental comparison [19] performed in terms of acceleration and stress state on a system configuration with a test set-up with both masses equal to 52 g (Fig. 1). By exciting the specimen in a frequency range from 600 to 850 Hz it showed a natural frequency equal to 771 Hz. In Fig. 3, it is easy to verify the goodness of the comparison between experimental and numerical results expressed in terms of PSD functions.

The present numerical activity has been performed with a different specimen set up (Fig. 2). The applied masses, showed in Fig. 2, have different values, as reported in Table 1 (mass no. 1 equal to 52 g and mass no. 2 equal to 156 g). In such way it was possible to excite more than one normal mode in a wider frequency range than the previous one [19].

The material parameters and geometrical dimensions of the specimen are all reported in Table 1.

The FE model was constrained at node 1 along all degrees of freedom, except the displacement in y-direction (Fig. 2). The input force was applied at the same node. Node 1 is connected by constraint equations rigidity to the lower base of the model, modelling the real test condition, in which the shaker excitation axis is not coincident with the specimen y principal axis.

The dynamic model was built by the modal state space approach described in Section 2.2, by considering a damping ratio ξ of 0.21%. All the information necessary to build the state space model were obtained by a modal analysis and are shown in Table 2. In Table 3 the modal stress shapes $[\Phi]^{\sigma}$ obtained by the same modal analysis for the most damage element is shown. It is necessary and sufficient to recover the stress state of this element using Eq. (15) after dynamic analysis was performed.

3.2. Input design and signals generation

Once the natural frequencies and mode shapes of the specimen are known, it was possible to design a correct input PSD function to excite one or more modes. By adopting the constrained condition and the excitation of Fig. 1, the first and the fourth modes showed to be the most suitable for the activity, being the most excitable by loads exerted along y-direction. These modes have natural frequencies of 196.97 Hz and 622.62 Hz respectively. Consequently, a constant flat PSD in the frequency range from 100 to 1500 Hz was used; see Fig. 4 for an input example with 6 N^2/Hz amplitude (that is, 91 N of RMS).

This experiment configuration allowed to perform the fatigue analysis on a multimodal model, extending the results previously obtained [19], in which only the fourth mode shape was excited, as well as with a wider set of non-stationary non-Gaussian inputs.

Starting from the ideal PSD (*i.e.* that of Fig. 4), several random loads with different RMS and kurtosis have been generated in order to certify under what circumstance it is possible to not consider the non-Gaussianity and non-stationarity of the input, approaching the problem of damage evaluation directly in frequency domain with the standard frequency domain methods. It has to be clarified that the linearity of the system leads to obtain just scaled values of the resulting stress when inputs with different RMS values are adopted. However, the choice to simulate various input RMS conditions is due to the will to follow the same experimental test campaign conducted in the previous paper and to prepare a numerical database to adopt for a future experimental campaign.

In order to generate all the signals used in this activity *i.e.* stationary and non-stationary with three different RMS value and with three different kurtosis 3, 5.5 and 7, firstly from the flat PSD function a stationary Gaussian load was generated with the indirect (time domain) method [31]. In fact, once a generic PSD function is given, a Gaussian time history can be computed by the following equation:

$$x(t) = \frac{1}{N}\sum_{k=1}^{N-1} C_x(k) e^{\frac{j2\pi k}{N}} \qquad k = 1,2,\ldots,N-1 \tag{26}$$

where $C_x(k)$ are the coefficient of the Fourier series. By re-arranging the Parseval theorem [1], it is possible to obtain the following equation:

$$2\sum_{k=1}^{N/2} |C_x(k)|^2 = 2\sum_{k=1}^{N/2} G(k\Delta\omega)\Delta\omega \tag{27}$$

from which it is possible to calculate the absolute value of $C_x(k)$.

To generate a random signal it is important moreover to choose the phase ϕ_k, mutually independent and uniformly distributed in the interval $[0,2\pi]$ so that the coefficient C_x are given by:

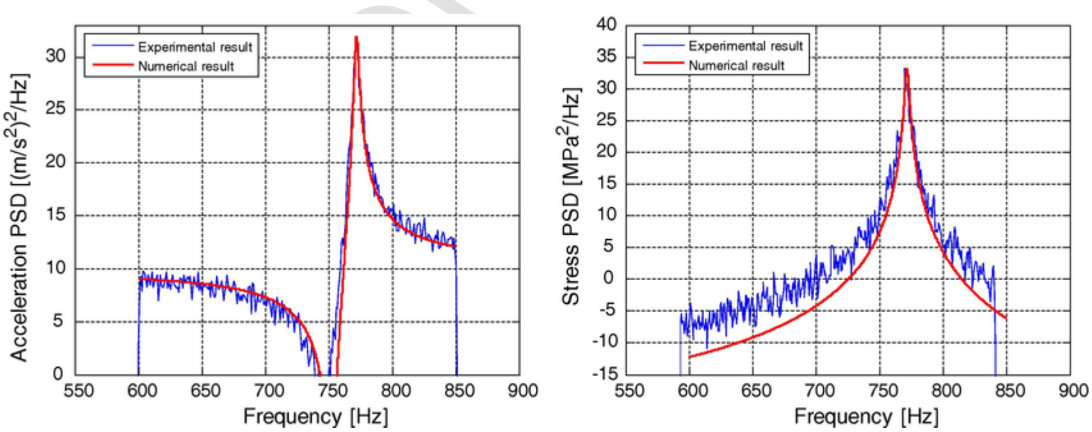

Fig. 3. Numerical model (FEM) validation by experimental comparison [19].

Table 1
Specimen characteristics.

Features	Unit	Value
Cross section	mm	10×10
Angle of Y-shaped specimen	degree	120
Mass 1	kg	$52 \cdot 10^{-3}$
Mass 2	kg	$156 \cdot 10^{-3}$
Young modulus	MPa	75,000
Density	$\mathrm{kg/m^3}$	2710
Fatigue exponent β	–	−0.169
Fatigue intercept α	MPa	987.5

Table 2
Natural frequency and input modal displacements of the specimen (Node ID 1).

Mode no.	$f_0\ [Hz]$	$[\Phi]^T_{inp}\ [m]$	ξ
1	196.97	0.107795	0.0021
2	208.93	$0.614584 \cdot 10^{-4}$	0.0021
3	386.51	$0.302328 \cdot 10^{-4}$	0.0021
4	622.62	0.209992	0.0021
5	1543.31	$0.169167 \cdot 10^{-7}$	0.0021
6	1548.26	$0.301467 \cdot 10^{-7}$	0.0021
7	1731.39	$0.457297 \cdot 10^{-8}$	0.0021
8	1777.49	$0.779448 \cdot 10^{-8}$	0.0021
9	1910.04	$0.106827 \cdot 10^{-5}$	0.0021

$$C_x(k) = |C_x(k)| e^{j\phi_k} \qquad k = 1,2,\ldots,N/2 \tag{28}$$

Once the coefficients are known, by (28) it is possible to generate a stationary Gaussian random signal.

The generation of stationary non-Gaussian loads is based on the assumption that a generic Gaussian process $x(t)$ is related to a non-Gaussian process $y(t)$ by:

$$x(t) = g(y(t)) \tag{29}$$

where g represents a transformation function. In this activity, the transformation function is that proposed by Winterstein [32,33] which is modelled as a monotonic cubic Hermite polynomial function. This method allows to estimate the transformation g from the first fourth central moments:

$$g = \frac{x-\mu}{\sigma} - \frac{s_k}{6}\left(\left(\frac{x-\mu}{\sigma}\right)^2 - 1\right) - \frac{k_u - 3}{24}\left(\left(\frac{x-\mu}{\sigma}\right)^3 - 3\left(\frac{x-\mu}{\sigma}\right)\right) \tag{30}$$

Once the transformation g is known, by computing the inverse of the transformation it is possible to determine the stationary non-Gaussian signal:

$$y(t) = G(x(t)) \qquad G = g^{-1} \tag{31}$$

The non-stationary non-Gaussian random loads instead have been generated by an amplitude modulation of a stationary Gaussian signal. The amplitude modulation carries out by a low frequency carrier wave $y(t)$ [14] independent from the Gaussian signals. In order to create large excursion, the amplitude of each cycle of the carrier wave is a random variable characterized by a β distribution [1,2]. The β distribution is chosen because it generates only positive value and it is extremely flexible. The mean value of the distribution is fixed to 0.5 and the variance is used to control the kurtosis. The parameters a and b of the β distribution are carefully chosen such that the kurtosis of the wave is one third of the required kurtosis. The non-stationary non-Gaussian signal can be easily obtained as follows:

$$z(t) = x(t) \cdot y(t) \tag{32}$$

where $z(t)$ represents the non-stationary non-Gaussian signal. Consequently, it is necessary to scale the obtained signal to the desired RMS.

All the input random signals, used in this activity to evaluate the non-Gaussianity and non-stationary effect on the fatigue life of a mechanical component, have been generated by the above techniques. 18 signals of 600 s length were generated, sampled at 12 kHz. The statistic characteristics of the random loads are stated in Table 4. In Figs. 5 and 6 some of these signals are shown. In particular, in Fig. 5 the stationary non-Gaussian inputs, characterized by the maximum RMS (input IDs 1, 4, 7 of Table 4), are represented. In Fig. 6, instead, the relative non-stationary ones are shown (test IDs 10, 13, 16). In Figs. 5 and 6 the PSD functions related to the time histories are compared with the ideal input PSD of Fig. 4. It is possible to observe that statistically very different (*e.g.* kurtosis, skewness, stationarity) signals result in very similar power spectral density.

3.3. Virtual tests with stationary loads

As stated in Table 4 nine different tests have been performed with stationary random loads with three different kurtosis and for three different RMS values. Once the time histories of the normalized coordinates q were obtained by transient dynamic simulation, the time histories of stress state $\{\sigma(t)\}$ were easily obtained by Eq. (13).

The uniaxial equivalent stress time history has been computed for each simulation and for each element of the model by the use of Braccesi et al. [17] method and an example of this result is shown in

Table 3
Stress modal shapes for the most damaged element (Element ID 1983).

Mode no.	$\sigma_x[Pa]$	$\sigma_y[Pa]$	$\sigma_z[Pa]$	$\sigma_{xy}[Pa]$	$\sigma_{xz}[Pa]$	$\sigma_{yz}[Pa]$
1	$0.114315 \cdot 10^{+11}$	$-0.806837 \cdot 10^{+11}$	0.00	$0.178330 \cdot 10^{+11}$	0.00	0.00
2	$-0.162358 \cdot 10^{+11}$	$-0.623562 \cdot 10^{+12}$	0.00	$-0.110424 \cdot 10^{+12}$	0.00	0.00
3	$-0.396252 \cdot 10^{+11}$	$0.389701 \cdot 10^{+11}$	0.00	$-0.780237 \cdot 10^{+11}$	0.00	0.00
4	$-0.312617 \cdot 10^{+12}$	$-0.235918 \cdot 10^{+13}$	0.00	$-0.297625 \cdot 10^{+11}$	0.00	0.00
5	$0.365068 \cdot 10^{+7}$	$-0.384445 \cdot 10^{+7}$	0.00	−91980.1	0.00	0.00
6	$0.138246 \cdot 10^{+8}$	160623	0.00	−577244	0.00	0.00
7	$0.179470 \cdot 10^{+8}$	$0.992324 \cdot 10^{+7}$	0.00	209685	0.00	0.00
8	$-0.250958 \cdot 10^{+9}$	$-0.271874 \cdot 10^{+9}$	0.00	$0.131871 \cdot 10^{+7}$	0.00	0.00
9	$0.126075 \cdot 10^{+9}$	$0.134044 \cdot 10^{+10}$	0.00	$0.142942 \cdot 10^{+7}$	0.00	0.00

UNCORRECTED PROOF

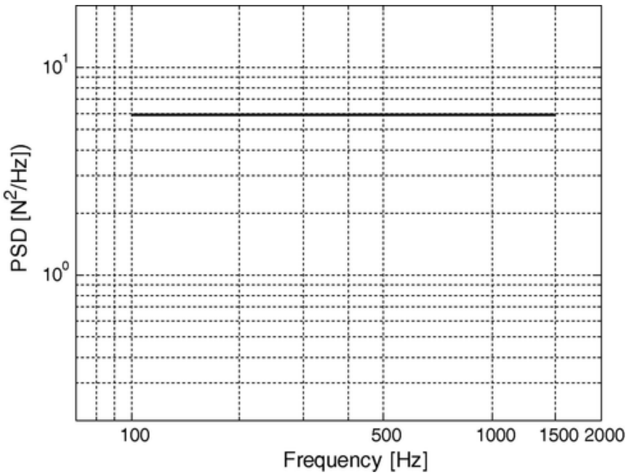

Fig. 4. Input PSD function.

Table 4
Input loadings characteristics.

Test ID	Input signal	rms $[N]$	k_u	s_k
1	Stationary	91	2.99	$-3.42 \cdot 10^{-4}$
2	Stationary	62	2.99	$-3.42 \cdot 10^{-4}$
3	Stationary	44	2.99	$-3.42 \cdot 10^{-4}$
4	Stationary	91	5.33	$5.26 \cdot 10^{-3}$
5	Stationary	62	5.33	$5.26 \cdot 10^{-3}$
6	Stationary	44	5.33	$5.26 \cdot 10^{-3}$
7	Stationary	91	6.67	$3.14 \cdot 10^{-5}$
8	Stationary	62	6.67	$3.14 \cdot 10^{-5}$
9	Stationary	44	6.67	$3.14 \cdot 10^{-5}$
10	Non-stationary	91	3.19	$3.84 \cdot 10^{-4}$
11	Non-stationary	62	3.19	$3.84 \cdot 10^{-4}$
12	Non-stationary	44	3.19	$3.83 \cdot 10^{-4}$
13	Non-stationary	91	5.38	$-1.41 \cdot 10^{-4}$
14	Non-stationary	62	5.38	$-1.41 \cdot 10^{-4}$
15	Non-stationary	44	5.38	$-1.41 \cdot 10^{-4}$
16	Non-stationary	91	7.04	$8.15 \cdot 10^{-3}$
17	Non-stationary	62	7.04	$8.15 \cdot 10^{-3}$
18	Non-stationary	44	7.04	$8.15 \cdot 10^{-3}$

Fig. 7 where the equivalent stress processes obtained for the most damaged element (Element ID 1983) for Test IDs 1, 4 and 7 were represented together with the relative distributions (histograms).

By observing Table 5, in which the output signals statistics are shown, the output kurtosis k_u of the uniaxial-equivalent stress for the most damaged element is always around 3, attesting how in case of stationary non-Gaussian excitation, also for a bimodal behaviour, the response of the system changes into stationary Gaussian. These results are furthermore confirmed by the non-Gaussianity coefficient λ_{ng} which assumes values always close to 1.

The fatigue life of the most damaged element has been evaluated in time domain by adopting the reference rainflow counting method [3] and Palmgren-Miner rule. The obtained results are shown in Table 5. As it is observable, the fatigue life for all the inputs characterized by the same RMS ($i.e.$44,62,91) are comparable to each other.

The fatigue life was evaluated also in frequency domain. To obtain the frequency domain stress representation, Eqs. ((14)–(17)) were adopted and the equivalent stress PSD of Premount [26] was evaluated. The fatigue life was obtained by Dirlik method [4] and Palmgren-Miner rule. These results are observable in Table 6. In Fig. 8 the Preumont stress PSD obtained for element ID 1983 and by considering the highest RMS input condition is shown. In this figure also the PSD functions of the Braccesi stress obtained for the relative time domain analysis are plotted to compare time domain with the frequency domain results. In particular, the result obtained in the Test IDs 7 and 16 (stationary and non-stationary input conditions with highest kurtosis value) are plotted.

As noticeable in Table 6, the estimated fatigue life in frequency domain is comparable to the same obtained in time domain.

For this reason, it is possible to state that in case of stationary excitations, the dynamics of the system takes an important role on the response. Indeed, in such condition the non-Gaussianity of the input can be omitted, and it is justifiable to perform frequency domain analysis attaining reliable results.

The probability density functions (PDF) and the cumulatives (CDF) of the equivalent uniaxial stress obtained in time and in frequency domain for the most damaged element (Element ID 1983) and for the simulation adopting the highest RMS value inputs are compared in Fig. 9.

3.4. Virtual tests with non-stationary loads

The damage evaluation was carried out also in case of non-stationary Gaussian inputs both in time and in frequency domain.

The response of the system to three different non-stationary inputs, with kurtosis 3,5.5 and 7, and three different RMS values (Table 4), was analysed. In such way it was possible to determine the importance of non-Gaussianity and non-stationarity of the inputs on the fatigue behaviour.

In Fig. 10 the time domain equivalent stress processes obtained for the most damaged element (Element ID 1983) for Test IDs 10, 13 and 16 were represented together with the relative distributions (histograms).

From Fig. 10 it is clear that at the non-stationary excitation, the system response maintains the statistic characteristics of the inputs. The output characteristics, for the most damaged element, are shown in Table 7. From these results it is possible to confirm that the kurtosis k_u of the uniaxial equivalent stress remains very similar to that of the input.

The fatigue life of the most damaged element has been evaluated in time domain by adopting reference rainflow counting method [3] and Palmgren-Miner rule. The obtained results are shown in Table 7: in case of non-stationary Gaussian inputs the obtained results are consistent with those obtained in the case of stationary loads. However, for the considered flexible specimen, in case of non-stationary non-Gaussian inputs the fatigue life is much shorter.

The fatigue life was evaluated also in the frequency domain. To obtain the frequency domain stress representation, Eqs. ((14)–(17)) were adopted and the equivalent stress PSD of Premount [26] was evaluated. The fatigue life was obtained by Dirlik method [4] and Palmgren-Miner rule.

In Fig. 8 the Preumont stress PSD obtained for element ID 1983 and by considering the highest RMS input condition is compared with time domain result. In particular, the result obtained in a non-stationary test (Test ID 16) is shown.

The probability density functions (PDF) and the cumulatives (CDF) of the equivalent uniaxial stress obtained in time and in frequency domain for the most damaged element (Element ID 1983) and for the simulation adopting the highest RMS value inputs are compared in Fig. 11.

From results stated in Table 8, no difference is appreciable in terms of fatigue life computed by time and frequency domain approach for the case of non-stationary Gaussian excitations. This results can be explained by the stationarity of the stress response (Fig. 10).

UNCORRECTED PROOF

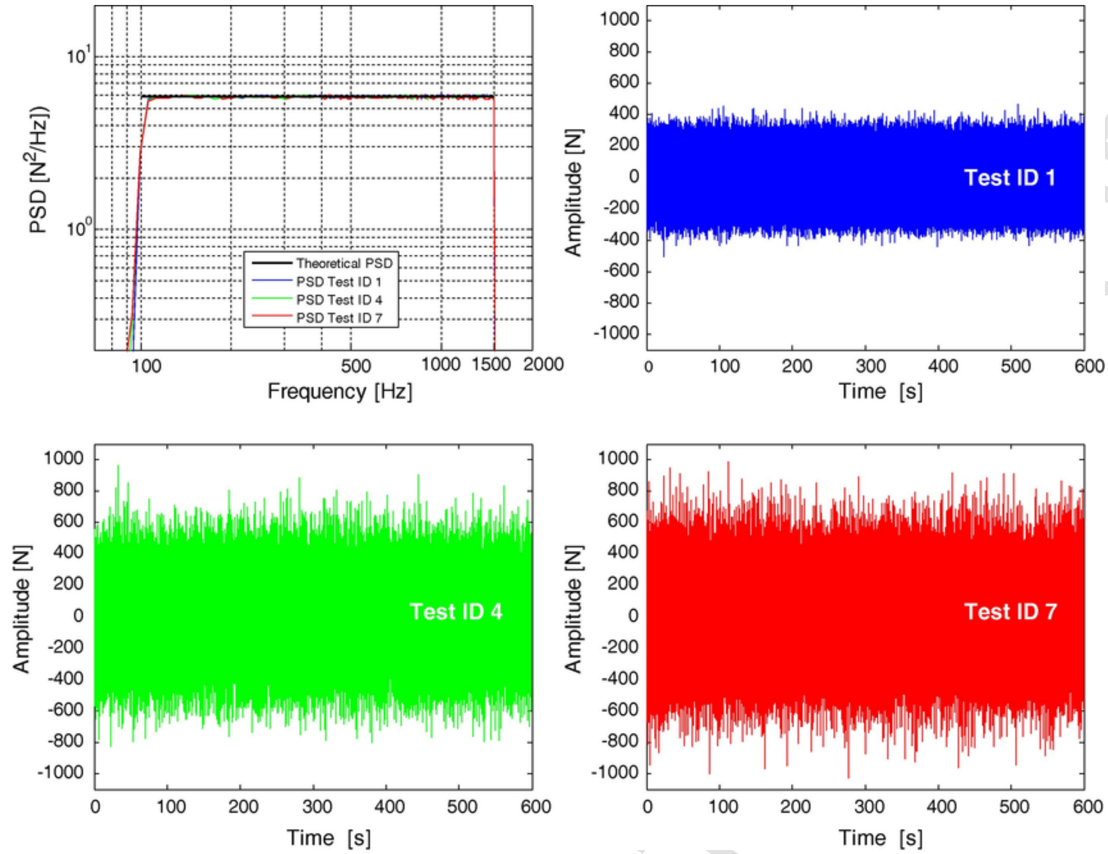

Fig. 5. Stationary inputs. Representation of some input time histories (Test IDs 1, 4, 7 of Table 4) and of their PSD functions compared with the ideal input PSD (Fig. 4).

By comparing the calculated results in frequency domain (Table 8) with the fatigue life obtained in time domain under non-stationary non-Gaussian condition, the difference is evident. This results arises from the non-stationarity and non-Gaussianity of the stress response (see Fig. 10). In fact, the frequency methods such as the Dirlik [4] do not take into account the high excursion peaks which are the cause of the higher cumulated damage within the structure.

Results shown in Fig. 12 shows the corrected fatigue damage as proposed by Braccesi et al. [17]. The non-Gaussian coefficient λ_{ng} was calculated for each test condition. The computed values are stated in Table 7, in which it is possible to note as for the case of non-stationary Gaussian excitations the λ_{ng} is closed to 1, while for the case of non-stationary non-Gaussian excitation, the correction coefficient ranges from 7.58 to 14.61.

The fatigue life shown in Fig. 12 and in Table 8 demonstrates that the proposed approach, that is the frequency domain evaluation of the damage and correction of it by coefficient λ_{ng}, gives reliable fatigue life estimation at (non-) Gaussian or (non-) stationary excitation.

4. Conclusion

The aim of this activity was to demonstrate that it is possible to correctly foresight, by numerical modelling and simulation, the dynamic behaviour of linear systems excited by non-Gaussian and non-stationary loading conditions, and, consequently, the statistical distribution of the generic outputs (i.e. deformations, accelerations, stresses, strains).

Starting from an experimentally validated numerical modelling and simulation methodology (by FE and State-Space approaches), the response of a simple linear model, representing a real component adopted in a previous experimental activity, was analysed by exciting the FE model with a set of several stationary and non-stationary time domain input signals (loads) characterized by statistical distributions affected by high kurtosis (with skewness equal to 0).

It has been verified as the linear state space modelling and simulation is able to perceive the modulation of the input statistical contents in the same manner as it was observed during the experimental activity.

In particular, in this paper the research was aimed to analyse the multi modal behaviour, that is the conditions in which more than one mode was involved into the system response.

It has been demonstrated that if the system is excited with a stationary input loading in the frequency range of one of its modes or natural frequencies, the response of the system is always Gaussian even if the input is strongly non-Gaussian (i.e. high kurtosis values). Such phenomenon can be observed both in case of one or more excited modes.

Such results allow to address the analysis to a simpler simulation condition: in case of stationary non-Gaussian loading conditions, if the frequency content affects the system dynamics, it is possible to state that the damage evaluation can always be performed under the hypothesis of Gaussianity i.e. adopting the frequency domain approach, obtaining accurate results with shorter computational time if compared to the classical time domain analysis.

Instead, it has been observed that in case of non-stationary non-Gaussian excitations for the particular considered specimen, the response of the system remains non-Gaussian and non-stationary with high kurtosis values. In this case it is not allowed a simulation condition based on the hypothesis of Gaussian outputs. Indeed, the re-

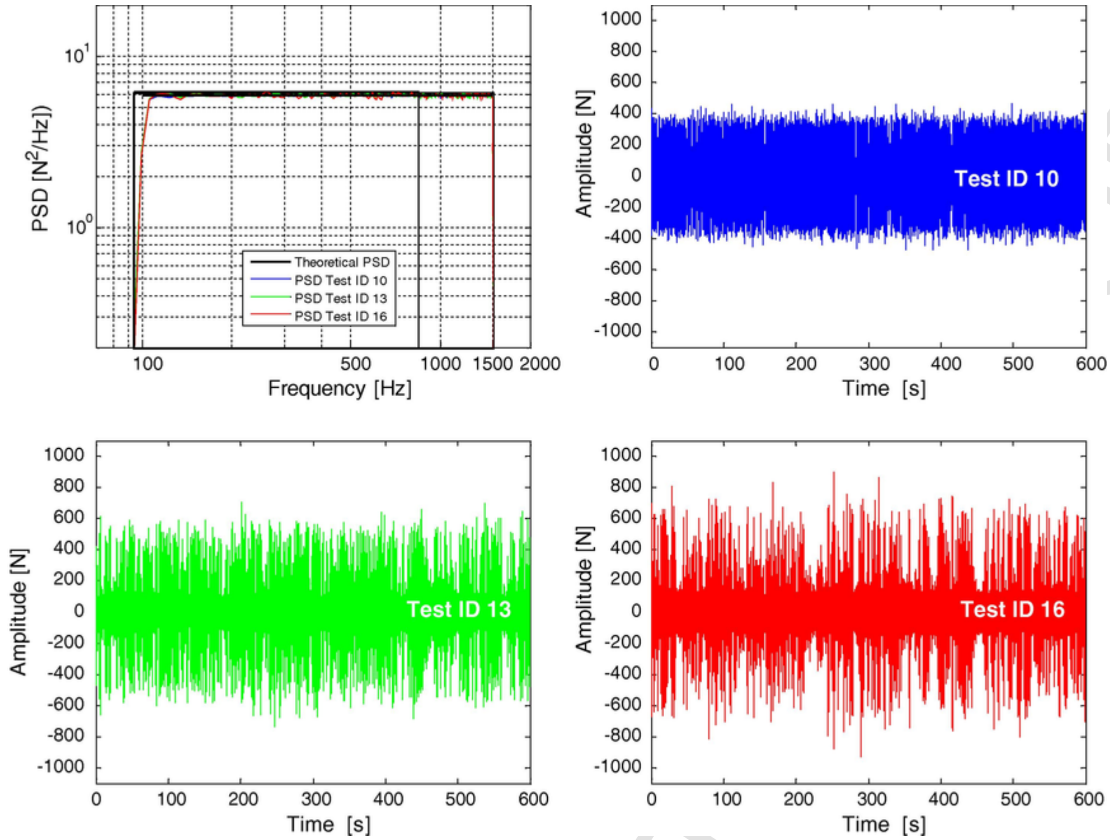

Fig. 6. Non stationary inputs. Representation of some input time histories (Test IDs 10, 13, 16 of Table 4) and of their PSD functions compared with the ideal input PSD (Fig. 4).

sponse of the system is always non-Gaussian and characterized by high kurtosis values close to that of the input signal.

It has been demonstrated that a smart solution of the problem of fatigue damage evaluation in case of non-stationary non-Gaussian excitations is a frequency domain analysis combined with the damage correction method proposed by the authors. Indeed, this approach guarantees accurate results with short computational time of dynamic simulation and cycles counting evaluation.

This approach is based on the kurtosis and skewness (in this case equal to zero) of the stress state values and on the fatigue strength curve slope. The use of such method needs however a short transient analysis aimed to evaluate the kurtosis and the skewness of the stress response.

The effectiveness of this method was demonstrated by a numerical comparison between the reference results (obtained by transient dynamic simulations and Rainflow counting method) and those obtained by the proposed approach.

Moreover, it has been observed that in case of strongly non-stationary non-Gaussian excitations, the output kurtosis value is closed to that of the inputs loading. This result makes the correction method faster than the reference one, since the correction coefficient can be computed by the kurtosis and the skewness values of the inputs.

The obtained damage values are obviously an approximation of the real one, but in the preliminary design phases this methodology allows to save time guaranteeing accurate results.

UNCORRECTED PROOF

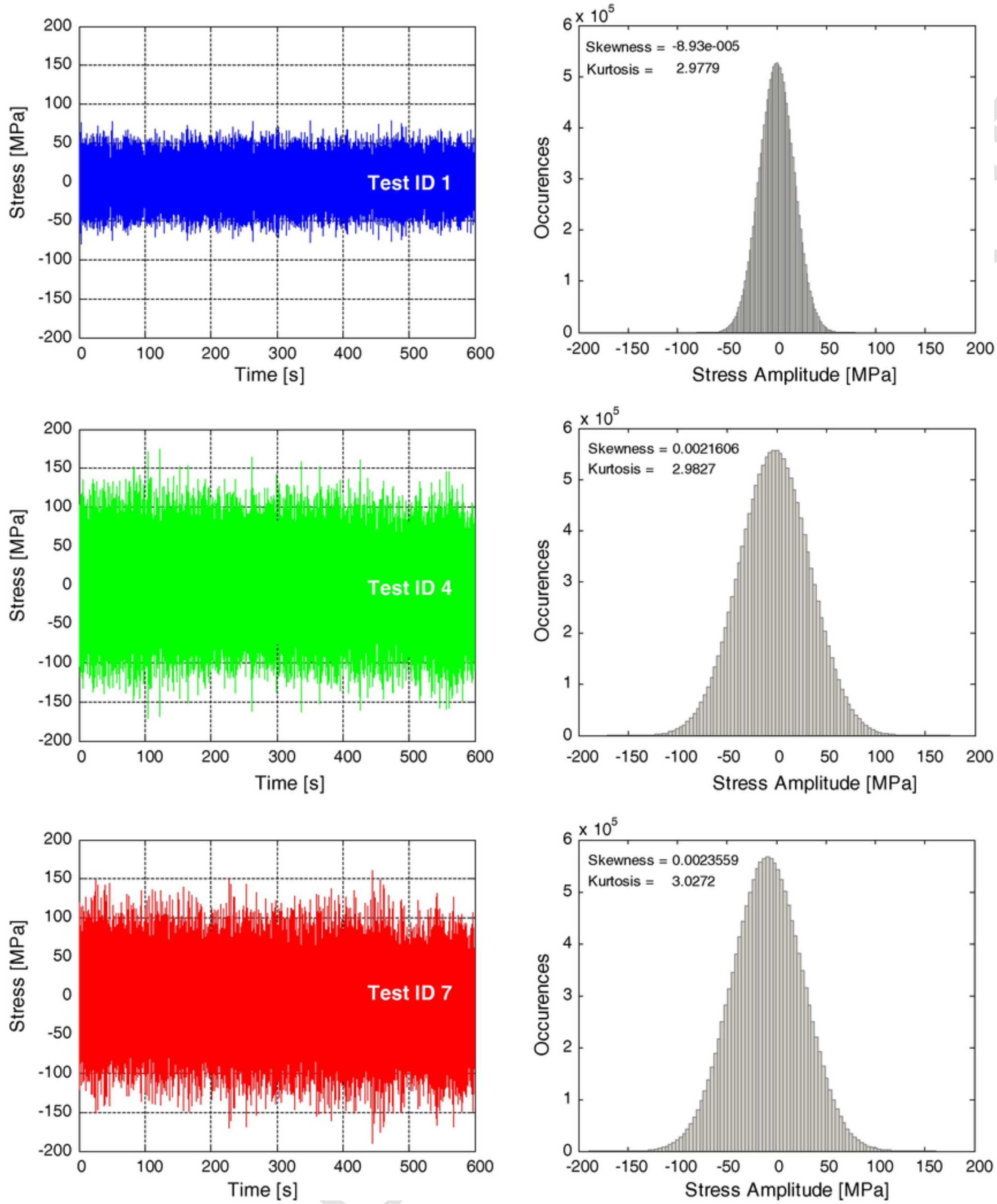

Fig. 7. Stationary inputs. Representation of some output time histories (left column) of uniaxial equivalent stress for Element ID 1983 (Test IDs 1, 4, 7 of Table 4) and of their relative distributions (histograms).

Table 5
Fatigue Life in time domain and output characteristics for stationary loadings (Element ID 1983).

Test ID	Input k_u	Output rms $[MPa]$	Output k_u	Output s_k	Corr. Coeff. λ_{ng}	Life $[s]$ (Rainflow)
1	2.99	36.0113	2.9779	$-8.93 \cdot 10^{-5}$	0.9818	$4.64 \cdot 10^{+4}$
2	2.99	24.5352	2.9779	$-8.93 \cdot 10^{-5}$	0.9818	$3.89 \cdot 10^{+5}$
3	2.99	17.2372	2.9779	$-8.93 \cdot 10^{-5}$	0.9818	$2.61 \cdot 10^{+6}$
4	5.33	35.6505	2.9827	$-2.61 \cdot 10^{-3}$	0.9857	$5.08 \cdot 10^{+4}$
5	5.33	24.2894	2.9827	$-2.61 \cdot 10^{-3}$	0.9857	$4.26 \cdot 10^{+5}$
6	5.33	17.2372	2.9827	$-2.61 \cdot 10^{-3}$	0.9857	$2.85 \cdot 10^{+6}$
7	6.67	36.7604	3.0272	$2.35 \cdot 10^{-3}$	1.0228	$4.92 \cdot 10^{+4}$
8	6.67	25.0456	3.0272	$2.35 \cdot 10^{-3}$	1.0228	$4.12 \cdot 10^{+5}$
9	6.67	17.7742	3.0272	$2.35 \cdot 10^{-3}$	1.0228	$2.76 \cdot 10^{+6}$

Table 6
Fatigue life comparison for stationary loadings between time and frequency domain (Element ID 1983).

Test ID	Input k_u	Output k_u	Life $[s]$ (Rainflow)	Life $[s]$ (Dirlik)
1	2.99	2.9779	$4.64 \cdot 10^{+4}$	$4.52 \cdot 10^{+4}$
2	2.99	2.9779	$3.89 \cdot 10^{+5}$	$3.78 \cdot 10^{+5}$
3	2.99	2.9779	$2.61 \cdot 10^{+6}$	$2.53 \cdot 10^{+6}$
4	5.33	2.9827	$5.08 \cdot 10^{+4}$	$4.52 \cdot 10^{+4}$
5	5.33	2.9827	$4.26 \cdot 10^{+5}$	$3.78 \cdot 10^{+5}$
6	5.33	2.9827	$2.85 \cdot 10^{+6}$	$2.53 \cdot 10^{+6}$
7	6.67	3.0272	$4.92 \cdot 10^{+4}$	$4.52 \cdot 10^{+4}$
8	6.67	3.0272	$4.12 \cdot 10^{+5}$	$3.78 \cdot 10^{+5}$
9	6.67	3.0272	$2.76 \cdot 10^{+6}$	$2.53 \cdot 10^{+6}$

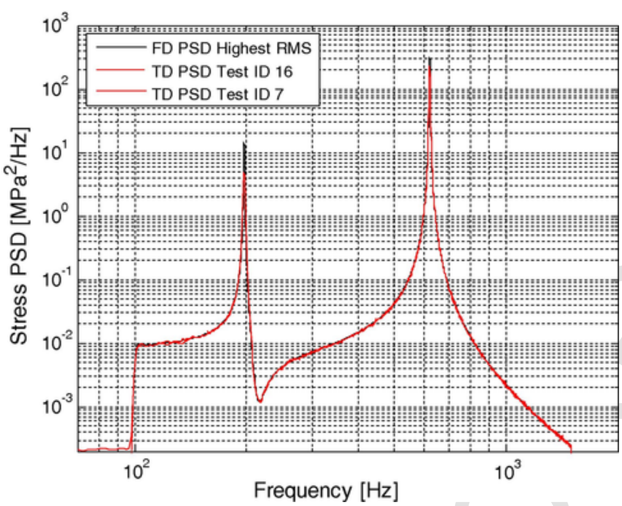

Fig. 8. Equivalent stress PSD functions. Comparison among frequency domain (FD) result (Preumont stress) and time domain (TD) ones (Braccesi stress). The results are obtained for element ID 1983, in the highest RMS input conditions.

UNCORRECTED PROOF

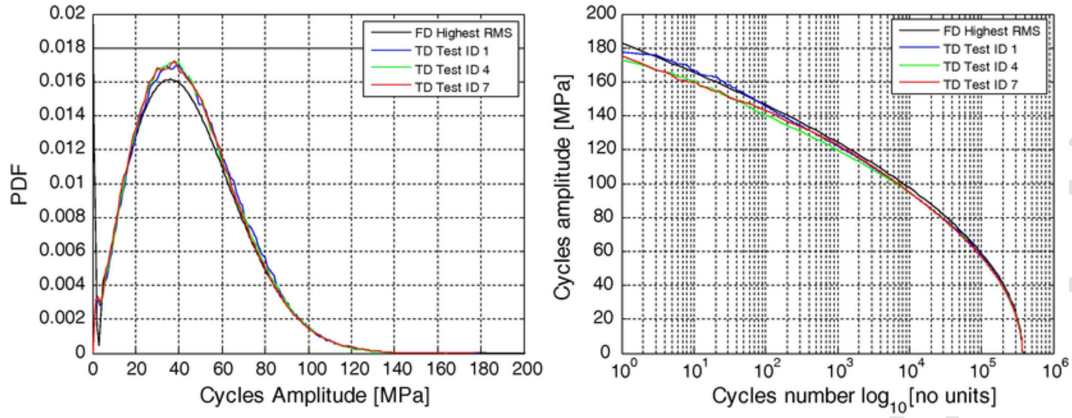

Fig. 9. Stationary inputs. Representation of PDFs of equivalent stress (left) and of CDFs (right) obtained in frequency domain (FD) and in time domain (TD) for Element ID 1983 in the highest RMS input conditions.

UNCORRECTED PROOF

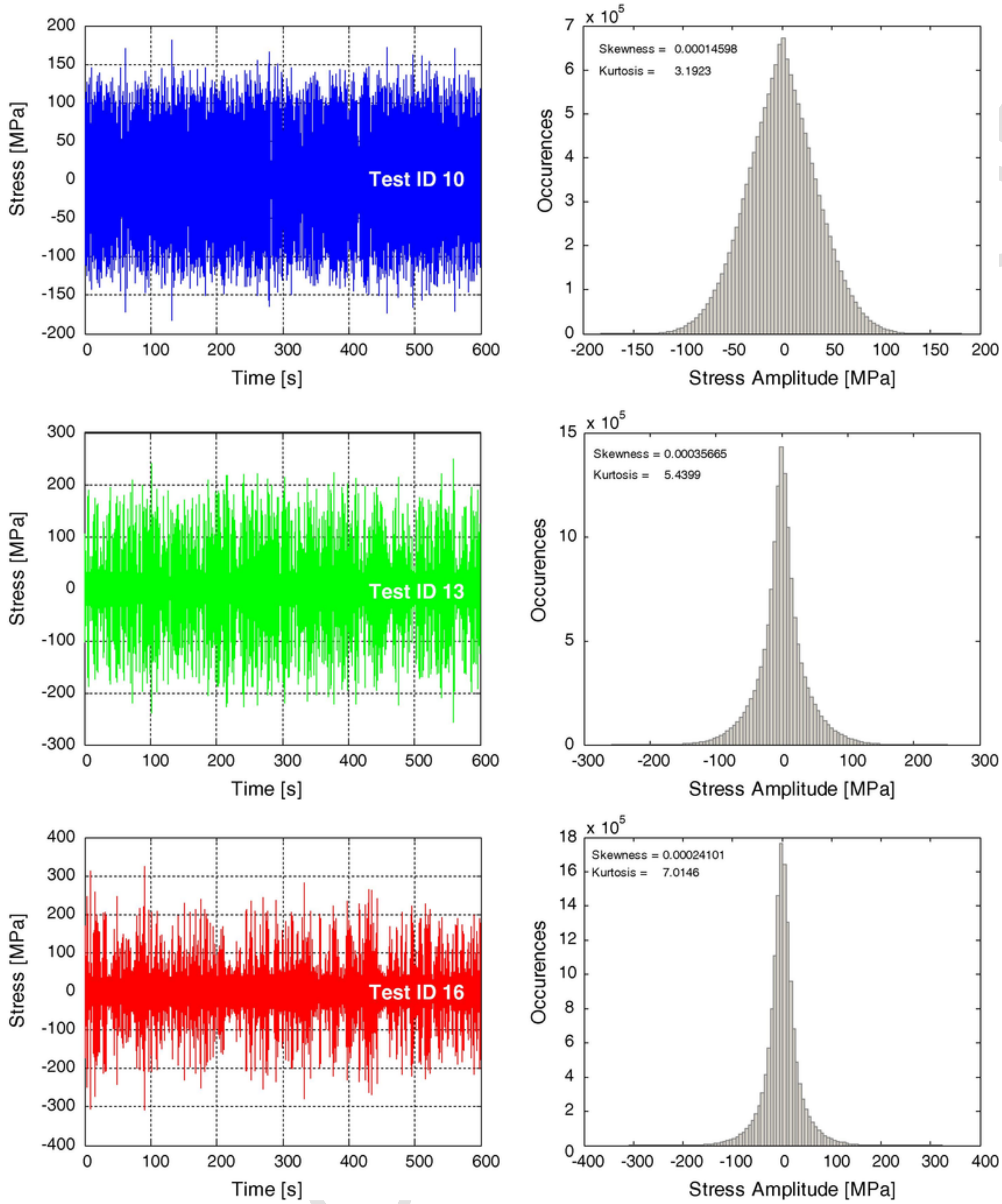

Fig. 10. Non stationary inputs. Representation of some output time histories (left column) of uniaxial equivalent stress for Element ID 1983 (Test IDs 10, 13, 16 of Table 4) and of their relative distributions (histograms).

UNCORRECTED PROOF

Table 7
Fatigue Life in time domain and output characteristics for non-stationary loadings (Element ID 1983).

Test ID	Input k_u	Output rms [MPa]	Output k_u	Output s_k	Coefficient λ_{ng}	Life [s] (Rainflow)
10	3.19	35.9612	3.1923	$1.46 \cdot 10^{-3}$	1.1731	$4.07 \cdot 10^{+4}$
11	3.19	24.5012	3.1923	$1.46 \cdot 10^{-3}$	1.1731	$3.41 \cdot 10^{+5}$
12	3.19	17.3878	3.1923	$1.46 \cdot 10^{-3}$	1.1731	$2.28 \cdot 10^{+6}$
13	5.38	36.6077	5.4399	$3.56 \cdot 10^{-3}$	7.5802	$1.29 \cdot 10^{+4}$
14	5.38	24.9415	5.4399	$3.56 \cdot 10^{-3}$	7.5802	$1.08 \cdot 10^{+5}$
15	5.38	17.7004	5.4399	$3.56 \cdot 10^{-3}$	7.5802	$7.25 \cdot 10^{+5}$
16	7.04	35.5047	7.0124	$2.41 \cdot 10^{-3}$	14.6124	$8.32 \cdot 10^{+3}$
17	7.04	24.2586	7.0124	$2.41 \cdot 10^{-3}$	14.6124	$7.26 \cdot 10^{+4}$
18	7.04	17.2158	7.0124	$2.41 \cdot 10^{-3}$	14.6124	$4.85 \cdot 10^{+5}$

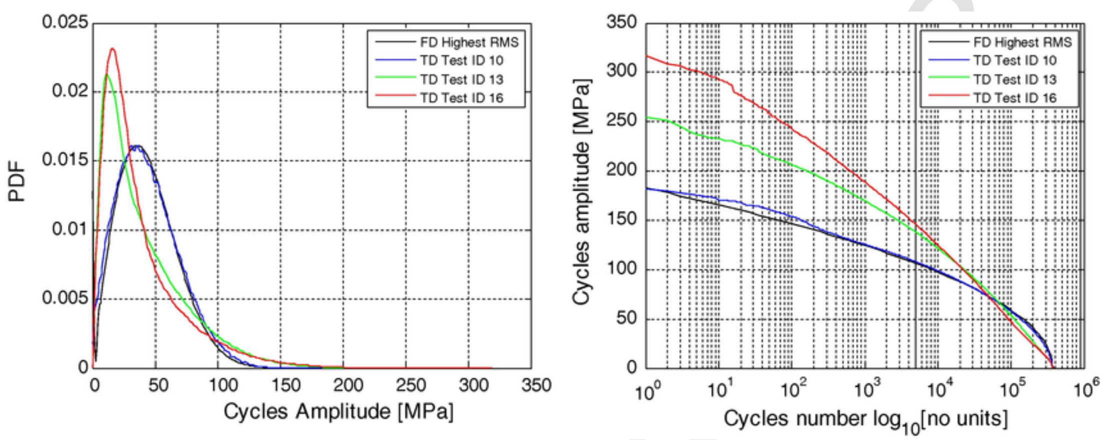

Fig. 11. Non stationary inputs. Representation of PDFs of equivalent stress (left) and of CDFs (right) obtained in frequency domain (FD) and in time domain (TD) for Element ID 1983 in the highest RMS input conditions.

UNCORRECTED PROOF

Table 8
Fatigue life comparison for non-stationary loadings between time and frequency domain (Element ID 1983).

Test ID	Input k_u	Output k_u	Life [s] (Rainflow)	Life [s] (Dirlik)	Corrected life [s] (Dirlik)
10	3.19	3.1923	$4.07 \cdot 10^{+4}$	$4.52 \cdot 10^{+4}$	$3.85 \cdot 10^{+4}$
11	3.19	3.1923	$3.41 \cdot 10^{+5}$	$3.79 \cdot 10^{+5}$	$3.23 \cdot 10^{+5}$
12	3.19	3.1923	$2.28 \cdot 10^{+6}$	$2.53 \cdot 10^{+6}$	$2.16 \cdot 10^{+6}$
13	5.38	5.4399	$1.29 \cdot 10^{+4}$	$4.52 \cdot 10^{+4}$	$5.96 \cdot 10^{+3}$
14	5.38	5.4399	$1.08 \cdot 10^{+5}$	$3.79 \cdot 10^{+5}$	$4.99 \cdot 10^{+4}$
15	5.38	5.4399	$7.25 \cdot 10^{+5}$	$2.53 \cdot 10^{+6}$	$3.34 \cdot 10^{+5}$
16	7.04	7.0124	$8.32 \cdot 10^{+3}$	$4.52 \cdot 10^{+4}$	$3.09 \cdot 10^{+3}$
17	7.04	7.0124	$7.26 \cdot 10^{+4}$	$3.79 \cdot 10^{+5}$	$2.59 \cdot 10^{+4}$
18	7.04	7.0124	$4.85 \cdot 10^{+5}$	$2.53 \cdot 10^{+6}$	$1.73 \cdot 10^{+5}$

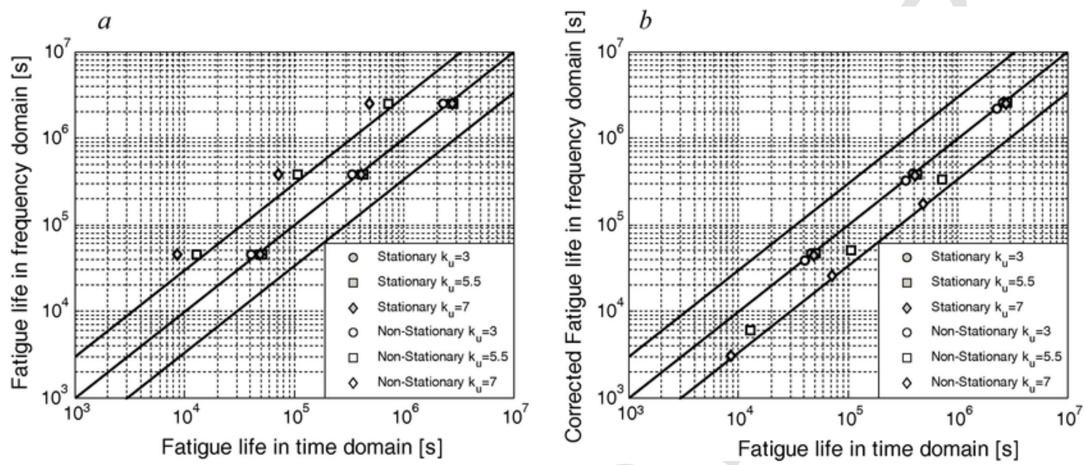

Fig. 12. Comparison of a) uncorrected and b) corrected fatigue life [17] (time vs frequency domain).

UNCORRECTED PROOF

References

[1] J.S. Bendat, A.G. Piersol, In: Random data: analysis and measurement procedures, 3rd ed.A Wiley Interscience Publication, 2000.
[2] A. Premount, Random vibration and spectral analysis, Kluwer Academic Publishers, 1994.
[3] W. Zhao, M.J. Baker, On the probability density function of rainflow stress range for stationary Gaussian processes, Int J Fatigue 14 (2) (1992) 121–135.
[4] T. Dirlik. Application of computer in fatigue analysis. PhD thesis. UK: University of Warwick; 1985.
[5] C. Braccesi, F. Cianetti, L. Tomassini, Random fatigue. A new frequency domain criterion for the damage evaluation of mechanical components, Int J Fatigue 70 (2015) 417–427.
[6] M. Wang, W. Yao, Frequency domain method for fatigue life analysis on notched specimens under random vibration loading, J Nanjing Univ Aeronaut Astronaut 40 (4) (2008) 489–492.
[7] V. Rouillard, M.A. Sek, The simulation of non-stationary vehicle vibrations, Proc Inst Mech Eng, Part D J Automobile Eng 215 (2001) 1069–1075.
[8] Amiri K, Mulu B, Raisee M, Cervantes MJ. Load variation effects on the pressure fluctuations exerted on a Kaplan turbine runner. In: Proceedings of 27th IAHR symposium on hydraulic machinery and systems (IAHR 2014), Montreal, Canada; 2014.
[9] Defense Standard 00-35. Environmental handbook for defense material. Part 5: induced mechanical environments; 1999.
[10] MIL-STD-810F. Department of defense test method standard for environmental engineering consideration and laboratory tests; 2000.
[11] Wolfsteiner P. Fatigue assessment of non-stationary random vibrations by using decomposition in Gaussian portions. Int J Mech Sci. Available online 3 June 2016 [in press].
[12] D.E. Newland, An introduction to random vibration and spectral analysis, 2nd ed., Longman Scientific and Technical, Essex (England), 1984.
[13] Rizzi SA, Prezekop A, Turner T. On the response of a non-linear structure to high kurtosis non-Gaussian random loadings. In: Proceedings of EURODYN2011 - 8th international conference on structural dynamics, Leuven, Belgium; 2011.
[14] Kihm F, Rizzi SA, Ferguson NS, Halppenny A. Understanding how kurtosis is transferred from input acceleration to stress response and its influence on fatigue life. In: RASD, 11th international conference, Pisa, Italy; 2013.
[15] D. Benasciutti, R. Tovo, Fatigue life assessment in non-Gaussian random loadings, Int J Fatigue 31 (4) (2009) 766–775.
[16] Benasciutti D. Fatigue analysis of random loadings. PhD thesis. Italy: University of Ferrara; 2004.
[17] C. Braccesi, F. Cianetti, G. Lori, D. Pioli, The frequency domain approach in virtual fatigue estimation of non-linear system: the problem of non-Gaussian state of stress, Int J Fatigue 31 (4) (2009) 766–775.
[18] A. Niesłony, M. Bohm, T. Łagoda, F. Cianetti, The use of spectral method for fatigue life assessment for non-Gaussian random loads, Acta Mechanica et Automatica 10 (2) (2016) 100–103.
[19] M. Palmieri, M. Česnik, J. Slavič, F. Cianetti, M. Boltezar, Non-Gaussianity and non-stationarity in vibration Fatigue, Int J Fatigue 97 (2017) 9–19.
[20] M. Mrsnik, J. Slavič, M. Boltezar, Multiaxial fatigue criteria for random stress response – theoretical and experimental comparison, Mech Syst Signal Process 76–77 (2016) 409–423.
[21] S.L. Grassie, Rail irregularities, corrugation and acoustic roughness: characteristics, significance and effects of reprofiling, Inst Mech Eng 226 (5) (2012) 542–557.
[22] W.L. Brogan, Modern control theory, Quantum Publishers Inc., 1974.
[23] C. Braccesi, F. Cianetti, Development of selection methodologies and procedures of the modal set for the generation of flexible body models for multibody simulation, Proc Inst Mech Eng Part K J Multi-Body Dynam 218 (1) (2004) 19–30.
[24] C. Braccesi, F. Cianetti, L. Tomassini, An innovative modal approach for frequency domain stress recovery and fatigue damage evaluation, Int J Fatigue 91 (2016) 382–396.
[25] C. Braccesi, F. Cianetti, G. Lori, D. Pioli, An equivalent uniaxial stress process for fatigue life estimation of mechanical components under multiaxial stress conditions, Int J Fatigue 30 (2008) 1479–1497.
[26] X. Pitoseit, A. Premount, Spectral methods for multi-axial random fatigue analysis of metallic structure, Int J Fatigue 22 (7) (2000) 541–550.
[27] G. Allegri, X. Zang, On the inverse power laws for accelerated random fatigue testing, Int J Fatigue 30 (6) (2008) 967–977.
[28] M. Mrsnik, J. Slavič, M. Boltezar, Frequency-domain methods for a vibration-fatigue-life estimation – application to real data, Int J Fatigue 47 (2013) 8–17.
[29] J.A. Collins, Failure of materials in mechanical design: analysis, prediction, prevention, Wiley & Sons, New York, 1993.
[30] O.H. Basquin, The exponential law of endurance test, Am Soc Testing Mater 10 (1910) 625–663.
[31] C. Braccesi, F. Cianetti, G. Lori, D. Pioli, Evaluation of mechanical component fatigue behavior under random loads: indirect frequency domain method, Int J Fatigue 61 (2014) 141–150.
[32] Smallwood DO. Generating non-Gaussian vibration for testing purpose. In: Proceedings of 74th shock & vibration symposium, Virginia Beach, VA; 2004.
[33] S.R. Winterstein, Nonlinear vibration models for extremes and fatigue, J Eng Mech 114 (10) (1988) 1772–1789.

UNCORRECTED PROOF

View publication stats